

Gamma Ray Emission from Radioactive Isobars

Severin Field

March 31, 2022

Abstract

Radioactive isobars are inherently unstable and prone to decay to reach a more stable state. Three of the forms of decay that can occur to stabilize one of these isobars are: beta decay, positron decay and electron capture. We take 5 different sources and measure the gamma ray energy spectrum to classify each sources decay scheme. We identified beta decay in $^{60}_{27}\text{Co}$ and $^{137}_{55}\text{Cs}$. We also identified electron capture in $^{57}_{27}\text{Co}$ and $^{54}_{25}\text{Mn}$ and lastly identified positron decay in $^{22}_{11}\text{Na}$.

I Introduction

The three types of decay schemes we will be looking for in gamma ray energy spectra are: beta decay, positron decay and electron capture.

I.I Beta Decay

Beta decay is the emission of a β particle (an electron) thus increasing the nuclear charge by one atomic charge unit. This happens through a neutron decaying into a proton and an electron. This also produces an anti-neutrino to conserve angular momentum. From here we are left with an excited state with two options for further decay. The first is simple gamma emission decay. Alternatively, the energy leftover from the nucleus decay can be transferred to an electron knocking it out of the K shell. This energy transfer appears as an x ray.

Beta decay is the decay from a neutron into an electron, proton and anti-neutrino.

$$n \rightarrow p + e^- + \bar{\nu}_e$$

Further, after the gamma emission, energy must remain conserved. This means that the energy must come from the mass difference between the parent and daughter nuclide.

$$E = M_n(Z, A) - M_n(Z + 1, A) - M_e \quad (1)$$

$$= M_a(Z, A) - M_a(Z + 1, A) \quad (2)$$

We can see in (2) that the energy released depends on the mass of a proton and the atomic mass.

I.II Positron Decay

In this scheme (scheme 2) a positron is emitted from the parent nuclide. In this process, a proton decays into a neutron, a positron which conserves the charge of the decay and a neutrino which conserves momentum.

$$p \rightarrow n + e^+ + \nu_e$$

Since the positron is anti matter, it is quickly annihilated with an electron. The energy released is in the form of gamma rays:

$$e^+ + e^- \rightarrow \gamma$$

To conserve momentum, a gamma ray must be emitted in both directions from the collision. The energy released is:

$$E_\gamma = M_e * c^2 = .511\text{MeV} \quad (3)$$

This makes positron emissions easy to identify in the gamma ray spectrum. There will be one dominant band at .511MeV because positrons annihilate quickly.

I.III Electron Capture

Our third decay scheme is described by an unstable nucleus capturing an electron to stabilize. This can be described by a proton and an electron merging to create a neutron and a neutrino to decay into a more stable state. In the case of isobars that undergo electron capture, there is an imbalance of protons and neutrons in the nucleus. This can be described by:

$$p + e^- \rightarrow n + \nu_e$$

Since the electron comes from the K shell of the atom, it is filled by an electron at a higher shell. This energy shift releases an X-ray. These can be identified by energy peaks between 0-100keV on the gamma ray spectrum.

Our goal is to identify the full gamma ray spectra of $^{57}_{27}\text{Co}$, $^{137}_{55}\text{Cs}$, $^{54}_{25}\text{Mn}$ and $^{22}_{11}\text{Na}$. All unstable radioactive isobars.

I.IV Detection

The Geiger counter is a popular method of measuring radiation, but one cannot precisely measure the direct energy of the incident particle with a machine that only beeps. This only detects the presence of particles. Another example of a detector is an NaI crystal doped with thallium. In this experiment, a Ge(Li) lithium drifted germanium detector is used. These have a much higher resolution than the NaI crystals and the ability to see the full spectrum as opposed to the Geiger counter. When a gamma ray enters the detector it produces a recoil electron by the photoelectric effect, Compton effect or pair production. Each type of event can be seen on the spectrograph.

In the photoelectric process, the output pulse is proportional to the energy of the gamma ray or x ray that produced the interaction. During this process gamma rays can knock an electron out of its current position opening an electron-hole for an electron from an upper layer to fill. This electron recoil creates the gamma ray or x ray recorded in our spectrum as photo peaks.

Another type of event is an electron-positron pair being created upon gamma ray absorption. These events can be noted on the spectrograph at energies above 1000keV because it takes roughly 1000keV to produce the mass of the two particles $E = 2M_e c^2 = 2 * 511\text{keV}$

I.V Compton Process and Compton Edges

Another process that can be seen on the spectrometer output is the Compton process. In this event, the gamma or X-ray is scattered by the recoil electron. The recoil electron absorbs some of the photons energy and if the scattered photon escapes from the detector then less energy is recorded. On spectra where the Compton process is dominant, there are a lot of particles detected at lower energies in a plateau because the energy is proportional to the degree of emission which is random. At the maximum, where the angle of emission is 180 degrees there is an edge called the Compton edge.

The plateau leading up to this edge is called the Compton plateau.

The equation for the energy transfer between an incident photon and an electron is

$$\frac{1}{E'} - \frac{1}{E} = \frac{1}{m_e c^2} (1 - \cos(\Theta))$$

Here E_{compton} is where the energy transfer releases the maximum energy:

$$E_{\text{compton}} = \max(E' - E) = E \left(1 - \frac{1}{1 + \frac{2E}{m_e c^2}} \right) \quad (4)$$

This is where we observe a Compton edge. In our analysis we will identify Compton edges and compare them to expected Compton edges using this formula.

II Experimental Procedure

II.I Instrumentation

In this experiment we use several different modules that are NIM (nuclear instrumentation module) standard. The NIM bin is where all of the electronic modules are housed. Our radioactive source is held in a metal tube next to the Germanium detector. (see I.IV) We use a high voltage supply and spectroscopy amplifier to turn on the detector. The Germanium crystal is kept cool with liquid nitrogen to avoid overheating. A pulser produces a steady stream of short pulses that stimulate a signal from the detector. The signal is read by an oscilloscope and read into our computer with a multichannel analyzer for data analysis.

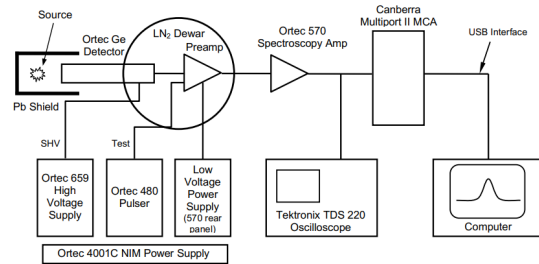


Figure 1: The entire configuration of the NIM and detector.

[1]

In an ideal detector, you get a sharp peak with counts only at the energy level of the event. Ge(Li) detectors come quite close to this and we get sharp peaks at relevant energy levels.

II.II Calibration

To calibrate the equipment, we use $^{60}_{27}\text{Co}$, a known isobar with a known output. We also send a pulser at a known energy level to measure the resolution of the instrument. At each photo peak is a gaussian, the peak energy and FWHM describe the energy released in the decay. Since we are given the known energy photopeaks of $^{60}_{27}\text{Co}$ (1.173MeV and 1.332MeV), we can confirm that the equipment is working correctly. Below is the output of our $^{60}_{27}\text{Co}$ decay:

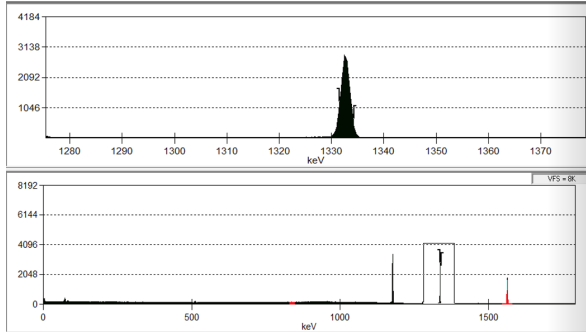


Figure 2: The spectra for cobalt 60 isotope. Above is the graph zoomed in on the second photopeak. The red peak is the pulser.

$^{60}_{27}\text{Co}$ follows the β decay scheme. The calibration curve is the channel plotted against the energy. Since all of the other decay schemes will fall within this one, we can set the channels (calibration) to match with these energies linearly. The two points on this curve are the two observed photopeaks. Since here there are roughly 8000 channels, the calibration goes as roughly 2MeV per 8000 channels.

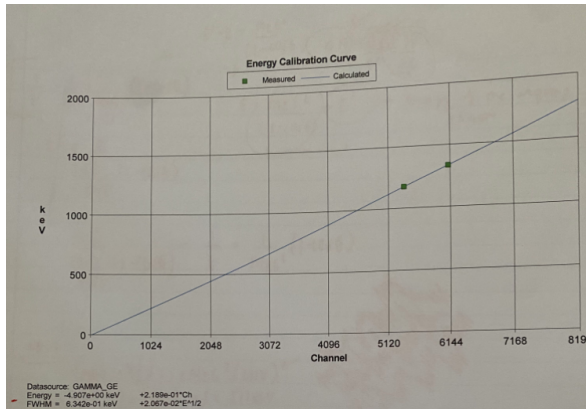


Figure 3: The calibration curve for the cobalt 60 isotope. There are 8000 bins (channels) that are now calibrated to measure events up to 2MeV

II.III Resolution

The $^{60}_{27}\text{Co}$ example also allows us to measure the resolution of the detector. The red peak in Figure 2 is not a photo peak but a pulser sent out by the electronics. The FWHM (full width at half maximum) of a photo peak corresponds with the resolution of the equipment, since ideally there should only be one discrete energy peak. Since the electronics and detector noise are uncorrelated they add in quadrature. The total resolution is:

$$(R_{\text{detector+electronics}})^2 = (R_{\text{det}})^2 + (R_{\text{elect}})^2 \quad (5)$$

Here the resolution is

$$R = \frac{\text{FWHM}}{\text{Photopeak}} \quad (6)$$

The total resolution is the sum of the squared detector and electronic component of the resolution. The electronics component can be found from the pulser peak which doesn't have to do with the detector. The total can be measured from the other photopeak. From there, the detectors resolution can be isolated.

From the calibration, the first photopeaks FWHM is 1.958keV and our pulser is 4.116keV. Equation 3 is now:

$$\left(\frac{4.116}{1559.4}\right)^2 = \left(\frac{1.958}{1172.2}\right)^2 + (R_{\text{det}})^2 \quad (7)$$

This leaves

$$R_{\text{det}} = 4\% \quad (8)$$

III Results and Analysis

III.I $^{22}_{11}\text{Na}$

The first radioactive isobar to look at is $^{22}_{11}\text{Na}$. The output spectra looks like:

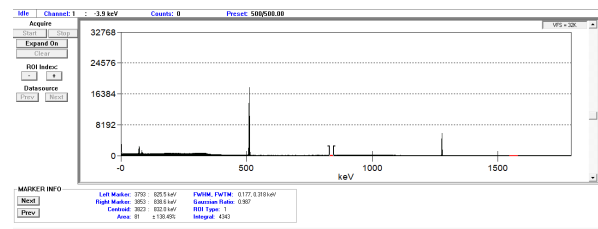


Figure 4: The sodium 22 isobar spectra

The $^{22}_{11}\text{Na}$ follows positron decay. This is because there is a very distinct peak that we measured at 505.4KeV, and it is the most discernible peak. In the positron decay scheme, two

positrons are emitted in each direction both with an energy of 511keV (from equation 3). This can explain the first peak. Clipping the data around a photopeak and putting it into python can find the uncertainty. With the Compton edge circled, this is what the emission spectrum looks like:

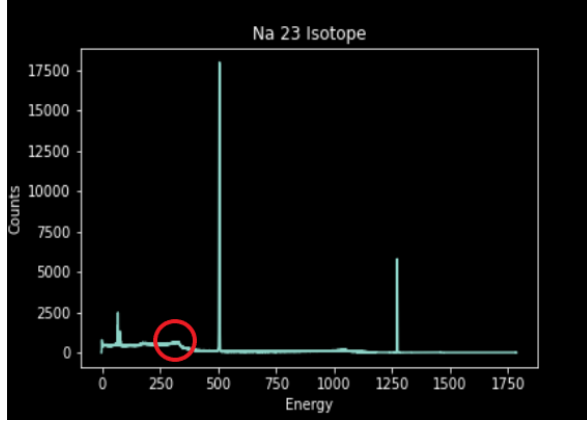


Figure 5: The sodium 22 isobar spectra

The first peak plotted in python looks like:

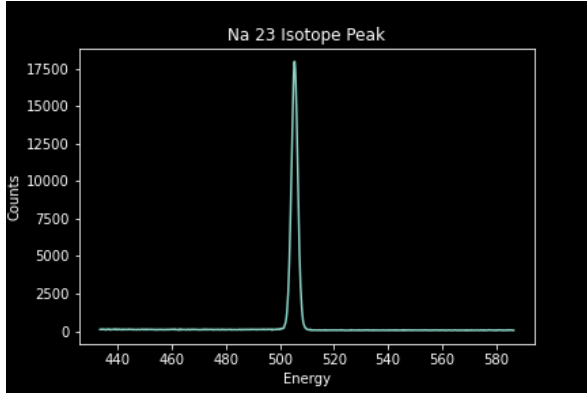


Figure 6: The sodium 22 isobar first peak

From this, there is an uncertainty of 1.66keV around the peak at 505.4keV. A github with all of the code used to generate every plot can be found in the references, this is just done by taking the energy values around 505 and running them through python's inherent standard deviation calculator.

The other peak is at 1272.8 with an uncertainty of 2.024keV. This is the gamma ray energy released when a proton decays into a neutron during positron decay. The second peak can be seen in figure 7.

In figure 5, I have circled the Compton edge.

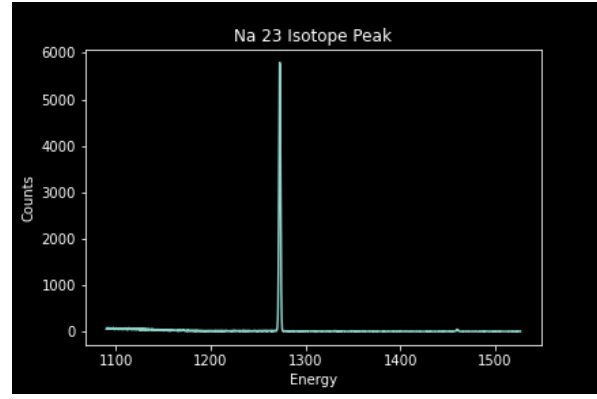


Figure 7: The sodium 22 isobar second peak

The experimental measurement for the Compton edge was at 335keV. The true Compton edge for a peak at 505.4keV can be calculated with equation 4 (see 9). Note the 505.4keV has been converted to $8.097e-14$ J to cancel SI units.

$$505.4keV * (1 - \frac{1}{1 + \frac{2*8.097e-14}{m_e c^2}}) = 335.54 \quad (9)$$

The observed Compton edge at 335keV matches the predicted Compton edge. The decay scheme for $^{22}_{11}Na$ can be seen below. It decays into $^{22}_{10}Ne$.

The nuclear energy level diagram can be described as follows:

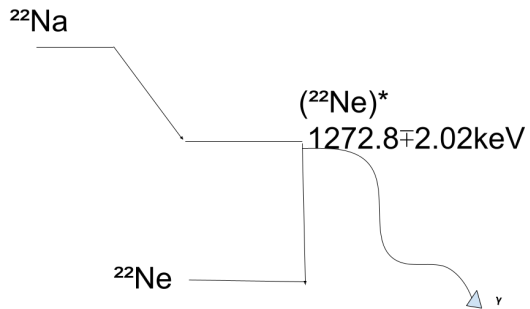


Figure 8: The sodium 22 nuclear energy diagram

III.II $^{57}_{27}Co$

The next radioactive isobar is $^{57}_{27}Co$. The output spectra looks like:

$^{57}_{27}Co$'s output spectra looks like electron capture. The spectrograph for this isobar was uniquely noisy

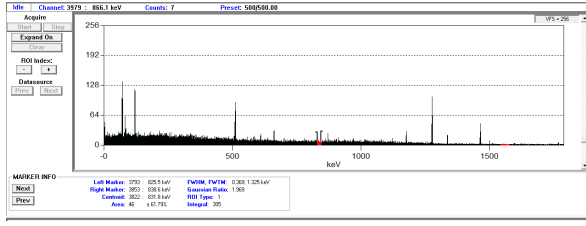
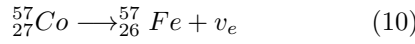


Figure 9: The cobalt 57 isobar spectra

but there is a distinct peak at 115.2keV and a lot of noise in the x-ray lower energies suggesting this is electron capture. The electron capture can be described by:



The most distinct peak with a Compton edge that we saw was at 115.2keV in figure 10. The Compton edge appears at $75.5 \pm 1.52\text{keV}$. The uncertainty we got using the same method as last time is 1.52keV.

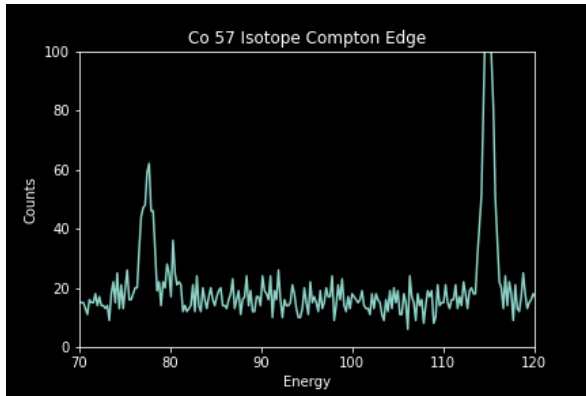


Figure 10: The cobalt 57 Compton edge. All of the graph creation code can be found in reference: [2]

The expected value can be calculated with:

$$115.2\text{keV} * \left(1 - \frac{1}{1 + \frac{2*1.846-14}{m_e c^2}}\right) = 35.7\text{keV}$$

This does not match the observation, either the Compton edge observed wasn't correct or we were measuring the Compton edge for the incorrect peak. The data is very noisy in the lower energies so it is difficult to identify clear Compton edges. This is because there are a lot of energy peaks.

The nuclear energy diagram can be seen in Figure 11.

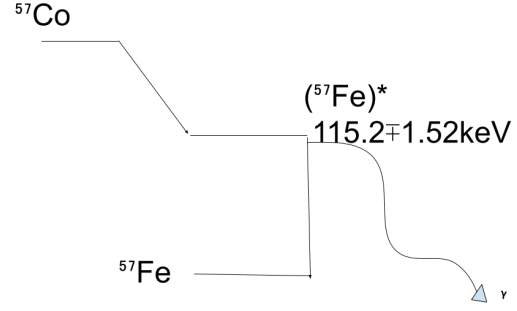


Figure 11: The Cobalt's nuclear energy diagram

III.III ${}^{54}_{25}\text{Mn}$

The next radioactive isobar we'll look at is ${}^{54}_{25}\text{Mn}$. The output spectra can be seen in Figure 12.

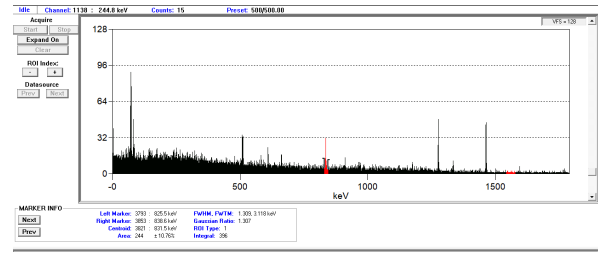


Figure 12: The manganese 54 isobar spectra

${}^{54}_{25}\text{Mn}$'s spectra looks like electron capture. This hypothesis matches the emission spectra because there is a lot of noise in the x-ray energies as well as a distinct peak. We see a clear peak at 66.5keV. The predicted Compton edge for this peak should be at:

$$66.5 * \left(1 - \frac{1}{1 + \frac{2*1.065-14}{m_e c^2}}\right) = 13.3\text{keV}$$

There is a Compton edge in the spectra for the peak at 1keV, but since there is so much noise from a lot of peaks it is difficult to see where the edges are.

This peak suggests that ${}^{54}_{25}\text{Mn}$ undergoes electron capture because it is an x-ray emission. The latter peaks show the energy released in decay.

The next peak at 1273.4 ± 1.332 to be the energy released in electron capture from the neutrino. The uncertainty here is just calculated with $.425 * FWHM$ of the peak. The expected Compton edge for this peak is at 1059.48keV. In the spectra there is a Compton edge around 1055.8keV. These results can yield a nuclear energy diagram. This can be seen in figure 14 below.

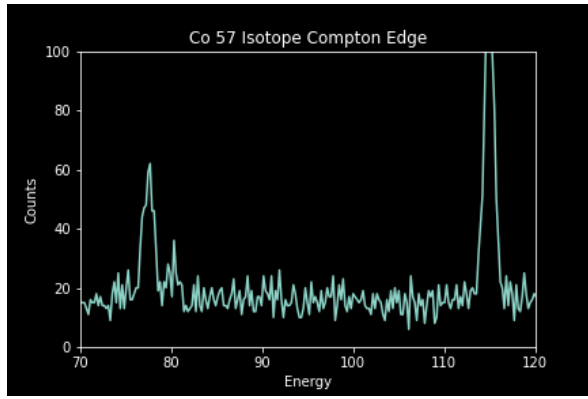


Figure 13: The MN54 Compton edge

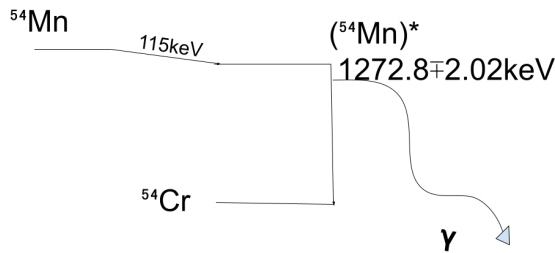


Figure 14: The Manganese 54 nuclear energy diagram

III.IV $^{137}_{55}\text{Cs}$

The next radioactive isobar is $^{137}_{55}\text{Cs}$. The output spectra can be seen in Fig

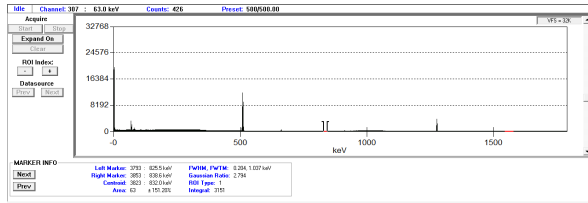


Figure 15: The cesium 137 isobar spectra

In this output (Figure 15) there are two photopeaks - one at 1024.3 ± 2.054 and another at 506.1 ± 2.758 . The uncertainty here is just the FWHM $\times .425$. The first Compton edge can be seen at 335, circled in Figure 16 below. The expected value for this Compton edge when plugged the energy peak

is plugged into Equation 4 is 336.16. The expected value for the second Compton edge is 819.47 and there is actually a Compton edge there that can be seen if you zoom in on the graph, but we did not record it during the experiment.

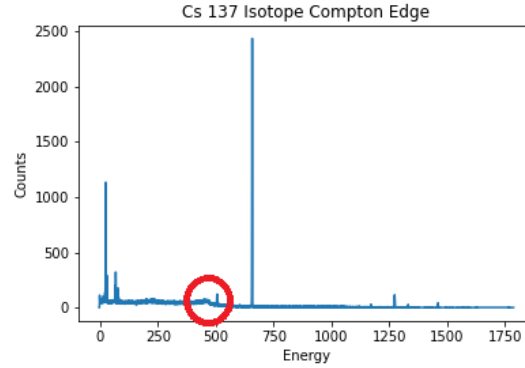


Figure 16: The cesium 137 isobar spectra with the Compton edge circled

We believe $^{137}_{55}\text{Cs}$ follows the Beta decay scheme, specifically, the 1b scheme where after gamma ray emission, the daughter is left in an excited state which eventually decays its new ground state.

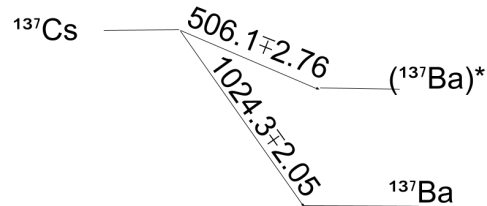


Figure 17: The cesium 137 Nuclear Energy Diagram

IV Conclusion

In this experiment we identified beta decay in $^{60}_{27}\text{Co}$ and $^{137}_{55}\text{Cs}$. We also identified electron capture in $^{57}_{27}\text{Co}$ and $^{54}_{25}\text{Mn}$ and lastly identified positron decay in $^{22}_{11}\text{Na}$. We did this by measuring the peak energies at photoelectric peaks from gamma ray radiation during nuclear decay. This told us the energy emitted in the transformations towards more stable

nucleii. In future experiments, we would like to isolate the source of noise in the $^{57}_{27}\text{Co}$ and $^{54}_{25}\text{Mn}$ output spectra and possibly calibrate the equipment better. I believe there was a systematic error in all of our results that we didn't notice until after losing access to the equipment. I think this had to do with the calibration because our results were systematically lower than they should've been. Below is a table of all of our recorded peaks.

Isotope	Peak 1	Peak 2
$^{57}_{27}\text{Co}$	115.2	
$^{60}_{27}\text{Co}$	1172.2	1332.55
$^{137}_{55}\text{Cs}$	506.1	1024.3
$^{54}_{25}\text{Mn}$	115	1272.8
$^{22}_{11}\text{Na}$	505.4	1272.8

References

- [1] W. Beyermann, *Gamma Ray Emissions from Unstable Isobars*. University of California, Riverside, 2022.
- [2] S. Field, “<https://github.com/sevdeawesome/gamma-ray>,” *University of California, Riverside*, 2022.